AD-A032 335

A Family of Finite Element Codes for the Analysis of Generalized Orthotropic Axisymmetric Bodies

Ballistic Research Labs Aberdeen Proving Ground Md

Oct 76

BRL MR 2697

BRL

MEMORANDUM REPORT NO. 2697

A FAMILY OF FINITE ELEMENT CODES FOR THE ANALYSIS OF GENERALIZED ORTHOTROPIC AXISYMMETRIC BODIES

William H. Drysdale

October 1976

USA BALLISTIC RESEARCH LABORATORIES
ABERDEEN PROVING GROUND, MARYLAND

Destroy this report when it is no longer needed.
Do not return it to the originator.

Secondary distribution of this report by originating or sponsoring activity is prohibited.

Additional copies of this report may be obtained from the National Technical Information Service, U.S. Department of Commerce, Springfield, Virginia 22151.

The findings in this report are not to be construed as an official Department of the Army position, unless so designated by other authorized documents.

1.b

UNCLASSIFIED
SECURITY CLASSIFICATION OF THIS PAGE (When Data Entered)

REPORT DOCUMENTATION PAGE		READ INSTRUCTIONS BEFORE COMPLETING FORM
1. REPORT NUMBER MEMORANDUM REPORT NO. 2697	2. GOVT ACCESSION NO.	3. RECIPIENT'S CATALOG NUMBER
4. TITLE (and Subtitle) A Family of Finite Element Codes For the Analysis of Generalized Orthotropic Axisymmetric Bodies		5. TYPE OF REPORT & PERIOD COVERED BRL MEMORANDUM 6. PERFORMING ORG. REPORT NUMBER
7. AUTHOR(s) William H. Drysdale		8. CONTRACT OR GRANT NUMBER(s)
9. PERFORMING ORGANIZATION NAME AND ADDRESS USA Ballistic Research Laboratory Aberdeen Proving Ground, Maryland 21005		10. PROGRAM ELEMENT, PROJECT, TASK AREA & WORK UNIT NUMBERS
11. CONTROLLING OFFICE NAME AND ADDRESS US Army Materiel Development and Readiness Command 5001 Eisenhower Avenue Alexandria, VA 22333		12. REPORT DATE October 1976 13. NUMBER OF PAGES 23
14. MONITORING AGENCY NAME & ADDRESS(if different from Controlling Office)		15. SECURITY CLASS. (of this report) UNCLASSIFIED 15a. DECLASSIFICATION/DOWNGRADING SCHEDULE

16. DISTRIBUTION STATEMENT (of this Report)

Approved for public release; distribution unlimited.

17. DISTRIBUTION STATEMENT (of the abstract entered in Block 20, if different from Report)

18. SUPPLEMENTARY NOTES

19. KEY WORDS (Continue on reverse side if necessary and identify by block number)

Stress Analysis, Finite Element, Orthotropic, Three-Dimensional Deformations, Filament Wound Fiberglass.

20. ABSTRACT (Continue on reverse side if necessary and identify by block number) (cee)

The SAGA family of finite element codes capable of analyzing axisymmetric bodies of filament wound composite materials (including torsional loads) is described. Changes made to the contractor supplied listings are discussed and the application of the codes to several example problems is presented.

DD FORM 1 JAN 73 1473 EDITION OF 1 NOV 65 IS OBSOLETE

UNCLASSIFIED
SECURITY CLASSIFICATION OF THIS PAGE (When Data Entered)

TABLE OF CONTENTS

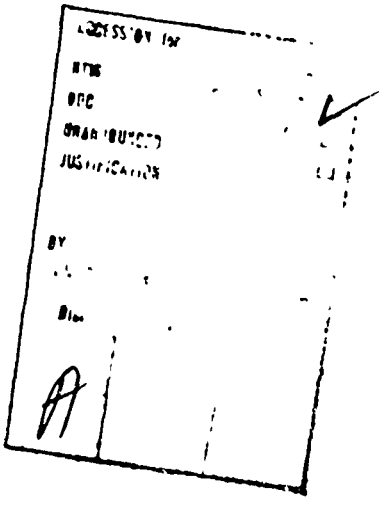

Preceding page blank

I. INTRODUCTION

One of the standard structural computer codes for elastic analysis used at BRL is a slightly modified version of the well known SAAS II.[1] This code performs stress analyses of axisymmetric structures (. one option, utilizing two-dimensional, ring-shaped, quadrilateral finite elements. It allows for non-isotropic material properties if the principal directions of the orthotropic material are oriented so as to preserve cylindrical symmetry. Among the more useful features of the SAAS II version at BRL is its automatic 2D mesh generator, which requires as input only the coordinates of certain boundary points.

The basic limitation of the SAAS II code is its two-dimensional character. This makes it inapplicable when torsional type loads,(e.g., torsional surface shear loading or angular acceleration,)are applied or when the principal axes of an orthotropic material are oriented at an angle to the axes of cylindrical symmetry. This latter exception would occur, for instance, in a filament wound composite pressure vessel with wrap angle other than 90^{0} (hoop winding). When BRL became involved in the analysis of fiberglass rocket launch tubes as part of the SMAWT program, the ability to model helical wrap angles other than 90^{0} on an exact, ply-by-ply basis became mandatory. The SAGA finite element code (for Stress Analysis of Generalized Axisymmetric Structures) was developed on contract by Prof. Adam Zak of the University of Illinois[2,3] primarily to meet this demand.

The new code was to be based on the existing SAAS II, retaining as closely as possible the same input format and mesh preparation so that users of the existing code would have no difficulty preparing runs for the new code. In addition, the logic would be similar. Two versions of the code were developed, the first retaining the straight-sided linear elements of SAAS and the second utilizing advanced quadratic isoparametric elements.

A detailed account of the two versions of the SAGA codes, along with listings and input instructions, may be found in References 2 and 3. This report will present a general description of the SAGA family of codes and discuss the modifications made to the contractor supplied programs. The application of these codes to some actual problems will be shown.

---

[1] *Sawyer, Stephen Gerard, "BRLESC Finite Element Program for Axisymmetric, Plane Strain, and Plane Stress Orthotropic Solids with Temperature-Dependent Material Properties," BRL Report No. 1539, March 1971.* (AD #727702)

[2] *Zak, Adam R., Second Quarterly Report, Contract No. DAAD05-73-C-0197, Ballistic Research Laboratories, Aberdeen Proving Ground, MD.*

[3] *Zak, Adam R., "Finite Element Computer Program for the Analysis of Layered, Orthotropic Structure," BRL Contract Report No. 158, June 1974.* (AD #783412)

II. DESCRIPTION OF THE SAGA CODES

The SAGA codes are designed for the linear elastic stress analysis of structures (the bilinear elastic option of the SAAS II code was dropped). The elastic material description used is that of an orthotropic material with nine independent elastic constants. The axes of material orthotropy are oriented at the angles α and β to the cylindrical coordinates as shown in Figure 1. This description is adequate to represent filament wound vessels exactly on a ply-by-ply basis. The orthotropic elastic material properties are then rotated automatically by the code in a rigorous tensor manner to obtain the properties in the cylindrical coordinates. For an arbitrary α and β, these properties are anisotropic rather than orthotropic, so that there is a coupling between normal and shear stresses and strains in all directions. SAAS II will accept as input only those material properties which are orthotropic in cylindrically symmetric directions. Hence, individual ply material properties must be approximately converted to cylindrically orthotropic properties manually prior to input. There can be no normal-shear coupling in this approximation. Since filament wound vessels are usually balanced by having α, the helical wrap angle, vary by plus and minus the same angle on alternate plies or groups of plies, the option to perform this type of variation automatically is included in the SAGA codes. The stress-strain relations allow for thermal strains and temperature dependent material properties, similar to SAAS II, but heat transfer problems are not solved in either approach.

The finite elements utilized for the representation of actual structures are annular elements with a quadrilateral cross section in the r-z plane. Each of these ring-shaped quadrilateral elements is formed from four triangular elements similar to the SAAS II code as indicated in Figure 2. The element forming subroutine has the capability to utilize triangular elements as a degenerate case, so that irregular boundaries may be fit more accurately. The locating of nodes for the elements is accomplished by the mesh generating subroutine of SAAS II, so that mesh input information is identical to that of the former code.

The geometric shape of the structure to be analyzed must be axisymmetric, in order to be modeled by annular elements. In addition, all loads applied to the structure are also axisymmetric. With this restriction the coordinate θ (see Figure 1) is not an independent variable. The strain-displacement relations used in the analysis are limited to this case.

The displacement pattern in each finite element allows full, three-dimensional deformations. In particular, the circumferential (hoop) displacement is not assumed to be identically zero. Along with this expanded displacement pattern, a general three-dimensional stress-strain field, independent of θ, results. Included in this field are the shear stresses $\tau_{r\theta}$ and $\tau_{z\theta}$, admitting torsion problems. The input boundary conditions were modified to allow for nodal parameter specification in three dimensions and to allow for torsional type shear loadings and angular acceleration inertial effects not found in SAAS II.

The output from the computer program consists of the displacements of the nodal points (in three directions) and the stresses and strains within each element. The stresses are presented first in the global cylindrical coordinate at each output point, and then, in terms of the principal material directions defined by the angles α and β. Because of this large amount of stress data, effective stresses are not computed in the SAGA codes.

An option in the SAGA codes allows the storage of the mesh and element data for a particular configuration. As a result, sequential computer runs with variation only in applied surface and inertial loads can be performed economically. This allows the loading to be applied incrementally to model quasi-static, time-dependent response in a more economic procedure.

This completes the general description of the common features of the SAGA codes. The two versions will now be considered.

SAGA I - Linear Version[2]

The term linear refers to the form of the shape functions used to describe the displacements within the triangular basic element. Since both versions of SAGA are isoparametric[4], this also means that the basic triangular element is linear; i.e., it has straight sides defined by the nodes at the apexes. Therefore, the mesh generator of the BRL version of SAAS II may be used directly for SAGA I and the element formation proceeds in an analogous manner.

Each of the nodes has three degrees of freedom (DOF) corresponding to displacements in the three coordinate directions. Four of the basic triangles are combined into a quadrilateral finite element as in Figure 2a. The degrees of freedom corresponding to the node in the center of the quadrilateral element are eliminated, using the equilibrium equations at that node, before the global stiffness matrix is formed. Stresses are output corresponding to the centroid of the quadrilateral element.

SAGA II - Quadratic Version[3]

The theory of higher-order isoparametric elements is outlined in Reference 4.

From a simplified point of view, quadratic elements imply that the unknown displacements are approximated by second-order shape functions within the basic triangular element. In addition, the sides of the element cross section are determined by quadratic curves; i.e., the element geometry is isoparametric ("iso" - equal, "parametric" - constants) to the displacement shape functions.

---

[4] *Zienkiewicz, O. C., Finite Element Method in Engineering Science, McGraw-Hill, New York, 1971.*

The finite elements are again ring-shaped, but the cross section of a typical element in the r-z plane may now have curved boundaries as in Figure 2b. In order to utilize the same mesh generator as that used in previous versions and still be capable of incorporating midside nodes, this finite element is constructed from the nodes corresponding to four elements of the linear versions of the code. This nodal location is indicated by broken lines in Figure 2b. Note that we must have an odd number of nodes in both directions. Since the mesh generator is capable of generating circular arcs, the element is able to represent a curved boundary as accurately as the grid is calculated. The mesh generator gives fairly uniform grids, so that there are no highly deformed boundary shapes for the element, a condition which must be satisfied for higher-order elements.[4]

The basic triangular element is formed from six nodes; the nodes at the apexes each have three degrees of freedom (DOF) corresponding to the three-dimensional displacement field, while the midside nodes have two DOF, corresponding to axisymmetric displacements only. This particular choice of displacement degrees of freedom was justified by the assumption that circumferential displacements are "more uniform" than the remaining ones and may be approximated by linear interpolation functions. This assumption reduces the total DOF of the basic triangular element by three. Each triangular element thus contains 15 DOF. The axisymmetric displacements are interpolated over the element from the values at six nodal points. The form of the shape function on the boundary is a quadratic function uniquely determined by the three nodal values lying on the boundary. Linear functions are used to interpolate the circumferential displacements from the apex nodal values. Having nodal points with different numbers of DOF requires careful logic and bookkeeping during total stiffness matrix and load vector formation.

Quadrilateral elements are formed from four basic triangular elements by eliminating all the degrees of freedom interior to the element. This elimination is accomplished by invoking equilibrium considerations for the common nodal points. The full quadratic quadrilateral element thus contains 20 DOF, as compared to the equivalent four linear elements, which contain 27 DOF (see Figure 3). This reduction in the number of DOF which must be considered for each element is one of the primary purposes for utilizing higher-order isoparametric elements.

The strains are calculated at four points within the quadrilateral element (located 80 percent of the distance along each diagonal from the centroid to the corner node) and these four values are used to interpolate the strain within the element at any position desired. The printout includes the stress and strain values calculated at the same spatial locations as those used in the linear version. This enables straightforward comparisons to be made.

III. MODIFICATIONS TO THE CODE

Minor changes to the computer program listings supplied by the contractor in References 2 and 3 for both versions of SAGA codes were necessary to implement the codes on BRLESC (the BRL electronic computer) and to correct bugs which appeared when inertial forces were considered.

Among the modifications necessary for code compatibility with BRLESC were:

a. A change in the dimension of alphanumeric arrays

b. The elimination of double precision specification cards (since BRLESC already uses the equivalent of double precision)

c. The elimination of mixed mode arithmetic

d. The change of some GO TO (i, j, • • •) statements (BRLESC will not handle a zero index value)

e. The elimination of indexed indices ; e.g., A(I(I)). In addition , the MPLOT subroutine was largely rewritten using BRLESC plotting commands.

Modifications provided by the contractor subsequent to the listing include the correction of an error in the mesh generator portion of the code. This error had been undiscovered in SAAS II. Also, two additional variables, KTL and KAT, were added to the POINTS subroutine to enable the code to handle large numbers of fiber orientation angles in setting up material property blocks. An option was added to the code to stop computation after only the mesh generating and initial plotting routines executed, in order to detect input errors before lengthy computation.

In the STRESS subroutine, before the strains in the element may be calculated, the displacements corresponding to the eliminated DOF must be found. The coding to accomplish this contained an error in both versions. For example, the quadratic version was

```
      DO  130 I   = 1, 11
      P (I+20)    = 0.0
      DO  130 J   = 1, 11
      DO  130 K   = 1, 20
130   P (I+20)    = P (I+20) + TR (I, J)*
                   (Q (J) - S(J+20, K) * P (K))
```

This procedure should calculate values for the eliminated displacements (P(21) thru P(31)) in terms of the known displacements on the boundary of the elements (P(1) thru P(20)), part of the partitioned stiffness matrix for the element (S (J + 20, K)), an inverted portion of the partitioned stiffness matrix (TR (I, J)), and the nodal forces acting on the eliminated nodes (Q (J)). However, in practice, this would effectively replace the nodal load by 20 times the load, due to the interior DO on K. This bug would appear only when Q (J) was nonzero; i.e., when inertial forces were present. This section of code was rewritten in the form

```
      DO  129  J = 1, 11
      DO  129  K = 1, 20
129 Q(J)       = Q(J) - S(J+20, K) * P(K)
      DO  130  I = 1, 11
      P (I+20)   = 0.0
      DO  130  J = 1, 11
130 P (I+20)   = P(I+20) + TR (I,J) * Q(J)
```

This correction eliminates the necessity of the code adjustment discussed in Ref 3, pg 16, which was required when inertial loads were present. The same considerations apply to the linear version of SAGA. During applications, the SAGA family of codes was found to require over an order of magnitude more computer time than the SAAS II code. This excessive run time was largely eliminated by a simple modification which will be discussed after the example problems have been presented.

In addition to the above modifications which apply to both versions, some changes were made to the quadratic version only. A section of the ISOSTF subroutine had been written to calculate the incremental stiffness matrix for a future non-linear version of the code, but was retained in the listing of the linear elastic code. It was deleted.

In the STRESS subroutine, the strains are found in the element at points located 80 percent of the distance along the diagonal from the centroid to the corners of the element and these values are used to interpolate the strain over the element. However, the coordinates of the corner nodes are used and interpolated with the same functions. To eliminate this discrepancy, the r and z coordinates of the points where the strain is found were calculated in ISOSTF when the strain matrix was formed and saved for use in STRESS.

For the purpose of computing the inertial forces in ISOSTF, the recomputation of the shape functions was eliminated. To calculate the rotational inertia force, the factor ω (angular velocity) was changed to ω^2. For the axial and tangential body forces, an excess R (radial distance) occurs (a factor R appears in the parameter XM). Finally, in the supplied listing, the calculated inertial forces were never added to the total element load vector.

Current listings of the codes, embodying all of the above changes, may be obtained from the author. No attempt will be made to list the two versions of the code in this report.

IV. APPLICATIONS OF THE SAGA CODES

The SAGA family of codes was tested on problems including a rotating disc, a pressure gage, and a charge design chamber.

a. Rotating Disc

In order to check the inertial capabilities of the codes, the simple problem of a rotating isotropic disc was analyzed. The disc had a radius of 12.7cm and was .635cm thick. The same nodal points were used for the grid on SAAS II, SAGA I, and SAGA II. A total of 63 nodal points were used, 21 along the radius of the disc and three through the thickness. The center row of 21 nodes was constrained against axial motion due to symmetry about the midplane. SAAS II and SAGA I divided the disc into two rows of twenty linear annular elements, while SAGA II used one row of ten quadratic elements. The stresses in the disc due to an angular velocity of 1000 rad/sec are shown in Table I. All codes gave a good approximation to a state of plane stress, with no z dependence of stress and small transverse values. The correct analytic values of the stress at r = .318 cm, based on plane stress assumptions, are σ_θ = 71 MN/m^2 and σ_r = 71 MN/m^2. There is excellent agreement among the codes for this example.

TABLE I. STRESSES IN ROTATING DISC

E = 10^6 psi (6.895×10^9 N/m^2) γ = .001 lb (mass)/in^3 (27.68 kg/m^3)
R = 5 inches (12.7 cm) ν = .3
t = .25 inches (.635 cm) ω = 1000 rad/sec

	SAAS II		SAGA I		SAGA II	
R in (cm)	$(\sigma_r/E)\times10^2$	$(\sigma_\theta/E)\times10^2$	$(\sigma_r/E)\times10^2$	$(\sigma_\theta/E)\times10^2$	$(\sigma_r/E)\times10^2$	$(\sigma_\theta/E)\times10^2$
.125 (.317)	1.0315	1.0320	1.0312	1.0315	1.0302	1.0307
1.13 (2.87)	.9791	1.0015	.9789	1.0012	.9785	1.0007
2.13 (5.41)	.8448	.9241	.8446	.9237	.8444	.9235
3.12 (7.92)	.6281	.7993	.6279	.7989	.6278	.7988
4.12 (10.5)	.3290	.6270	.3287	.6266	.3288	.6266
4.88 (12.4)	.0505	.4655	.0502	.4652	.0504	.4663
Total Computer Time	.84 min		9.05 min (Original Version)		15.1 min (Original Version)	

b. Pressure Gage

A second example, more detailed than the first, was used to compare the solutions to a problem which may be solved with SAAS II. Specifically, the problem is the analysis of an on-board pressure gage designed by H. Gay, formerly with BRL. The analysis of the gage with internal applied pressure and axial acceleration matching anticipated service conditions was performed by Arnold Futterer using SAAS II[5]. His finite element grid is shown in Figure 4. The same nodal points were used for the SAGA I and SAGA II calculations. The stress variation through the wall of the gage in the vicinity of the test section (near mid-length) is shown in Table II. The loads were a combination of 138 MN/m^2 internal pressure and an axial acceleration in the negative z direction of 8384 g. For this more complicated problem, the results are not as close as for the first example, but the variation between SAAS II and SAGA I is less than two percent. Since SAGA II utilizes more sophisiticated quadratic elements, it might be anticipated that for the same number of nodes this version of the code would yield superior results. The exact correspondence of SAGA II with the two linear codes would not be expected. The difference between the linear codes may be attributed to differences in round-off for the large number of equations to be solved since SAGA I must also eliminate the circumferential deflections during the equation solution process. The displacement output for both versions of SAGA did list all hoop deflections as zero, which should occur in this axisymmetric problem.

[5] *Futterer, Arnold, "Finite Element Analysis of Acceleration Effect on an Internal Ferrule Pressure Gage," forthcoming BRL Memorandum Report.*

TABLE II. STRESSES IN TEST SECTION OF PRESSURE GAGE

Internal Pressure = 20 kpsi (138×10^6 N/m^2)

E = 30×10^6 psi (207×10^9 N/m^2)

γ = .283 lb/in^3 (7830 kg/m^3)

Location Z = .305 in (.775 cm)

ν = .285

Axial Acceleration = 8384 g

r	SAAS II[5]		SAGA I		SAGA II	
	σ_θ(psi)	σ_θ(N/m^2)	σ_θ(psi)	σ_θ(N/m^2)	σ_θ(psi)	σ_θ(N/m^2)
.0979" (.249 cm)	38849	268×10^6	39193	270×10^6	39360	271×10^6
.1134" (.288 cm)	32003	221×10^6	32344	223×10^6	32452	224×10^6
.1289" (.327 cm)	27577	190×10^6	27907	192×10^6	27970	193×10^6
.1521" (.386 cm)	23456	161×10^6	23767	163×10^6	23861	165×10^6
	Total Computer Time = 4.6 min		Total Computer Time = 44.0 min (Original Version)		Total Computer Time = 49.2 min (Original Version)	

The computing time used by each code for these two examples has been indicated. The timer utilized by BRLESC does not have great precision, yet it may be seen that the SAGA family takes a factor of ten more run time than the SAAS II. This large increment in required computing time for the new codes would have seriously limited their potential usefulness. After being notified of this problem Professor Zak installed accurate timing procedures into the codes at the University of Illinois and was able to locate a single, inefficient, nested DO-loop in each of the SAGA codes. By rewriting this loop, the time savings indicated in Table III resulted. Similar time savings appeared in all other problems considered. Due to the increased number of unknowns, the solution of the linear equations should require 2.5 times more computer run time. The revised codes have the proper order of time required.

TABLE III. TOTAL COMPUTER RUN TIME ON BRLESC FOR THE GAY PRESSURE GAGE ANALYSIS

	SAGA I	SAGA II	SAAS II
Old Version	44.0 min	49.2 min	
			4.6 min
New Version	7.54 min	10.48 min	

Both versions of the SAGA code utilized the same nodal points. However, it may be seen that the increased number of eliminated variables in SAGA II did not result in a faster running program. This is undoubtedly due to the more detailed logic required to set up the elements and compute the desired stresses. However, the higher-order isoparametric elements may have better convergence properties so that fewer original nodal points are needed for a given accuracy. No comparisons on this point were made at this time, but evaluations will be made in the future.

c. Charge Design Chamber

An example of the unique capabilities of the SAGA code is demonstrated by the analysis of the design of the Charge Design Chamber. It is desired to have a model of a gun chamber within which a propellant may be ignited. The progression of propellant motion could be traced by the use of flash radiographs taken through the chamber walls. The chamber was to have a design pressure of 345 MN/m^2, but to be as thin as possible to retain maximum resolution for the flash radiograph records. It was decided that an S-glass fiber in an epoxy matrix would yield the highest X-ray visibility for the strength required. Filament wound fiberglass requires the type of analysis that the SAGA codes are intended to perform; i.e., non-cylindrically orthotropic material properties.

The interior dimensions of the chamber were determined by the dimensions of the gun chamber to be modeled. The chamber was approximately 101.6 cm long with an inner radius of 8.26 cm, incorporating a small linear taper toward the front of the chamber. Approximate calculations indicated that 44 plies of fiberglass windings .025 cm thick would be needed with the plies wound at alternate plus and minus angles of 64° to form 22 layers.

To model each ply with a single row of elements, a large number of elements are required through the thickness. Hence, the linear version was used for the analysis. Even with the SAGA I code, only some of the plies could be modeled individually; the remainder were grouped into elements several layers thick and the material properties approximated as cylindrically orthotropic.

The first attempt to model the entire chamber length with smaller elements near the ends resulted in the aspect ratio of some of the mid-length elements on the order of 170 to one; i.e., the elements were 170 times longer than thick. This led to a severe numerical instability in the equations formed, as was readily apparent from the solutions obtained. To avoid this difficulty, only segments of the chamber were analyzed at a time. It was found that reliable answers were obtained for aspect ratio as high as 50 to one over a chamber segment up to 30 elements long. These segments were primarily at the ends of the chamber so that the effects of the end mounting boundary conditions could be determined. Several design iterations of end constraint conditions were required to reduce the large bending moments in the chamber at these positions. A compressive prestress was imposed to reduce the possibility of "premature" hoop failure noted in some experiments.

Calculations revealed the stresses shown in Table IV for the chamber with ±64° degrees alternating plies away from the ends. The stresses shown are

TABLE IV. STRESSES IN CHARGE DESIGN CHAMBER

70% S-glass
30% resin

Material Properties of Fiber and Resin from Reference 6.

Internal Pressure = 50 kpsi ($345 \times 10^6 N/m^2$)

	All Plies ± 64°			6 inner plies ± 80°		
	σ_n	σ_s	σ_{ns}	σ_n	σ_s	σ_{ns}
Ply 1 (+)	402,118	-9,397	-65,426	437,807	-2,980	-19,359
Ply 2 (-)	400,343	-9,326	+65,246	436,004	-2,795	+19,295

[6] *Ashton, J. E., Halpin, J. C., and Petit, P. H., Primer on Composite Materials: Analysis, Technomic Publ, Stamford, Connecticut, Inc.*

those in the plane of the composite ply, with n indicating the direction of the fiber and s the direction normal to the fiber for the two inner plies where the fiber stress was maximum. The ultimate strength in the direction of the fibers is approximately 3100 MN/m^2 (from Reference 6). Hence, the fiber stress is within allowable limits. Likewise, the stress in the resin perpendicular to the fiber is compressive and allowable. This is information which could have been obtained from SAAS II by approximating a plus-minus ply combination by a single orthotropic layer. Based on this data alone the design appears to be adequate. However, the third column of the Table is the in-laminae (torsional type) shear, induced by anisotropic properties of material, a quantity which cannot be calculated by a two-dimensional code. This shear is well above the ply ultimate shear strength of approximately 138 MN/m^2, and would surely lead to the failure of the chamber.

The plies were rotated to hoop windings on all but the inner six plies, which were kept as helical windings of ± 80 degrees wrap angle to preserve some bending stiffness. Due to the greater stiffness to interior pressure of the hoop windings, six of the outer hoop plies could be removed leading to a thinner chamber wall. The stresses for this configuration are also shown in Table IV for the same position. The maximum σ_n occurs in the first hoop winding, but it is approximately equal to that in the inner ply. These predicted values are all less than the ultimate strength of the S-glass composite material.

Performing this design analysis with a code other than SAGA would not have revealed the high in-laminae shear of the original configuration and lead to the design of a chamber that would fail according to static failure criteria. (Rate and temperature effects on strength may also be important but are not considered in either approach).

d. Further Examples

The developer of the SAGA codes has applied the two versions of the codes to numerous simple examples and described the results of these investigations in Ref 2 and 3. Some of these examples have been duplicated at BRL to demonstrate machine transportability.

The application of the SAGA I code to the stress analysis of a portable, composite material, rocket launcher was performed by the contractor. The results of this analysis are presented in Reference 7. High values of in-laminae shear for helical wound fiberglass bodies are noted in this report also. No experimental verification of this analysis has been performed yet.

---

[7] *Zak, Adam R., "Numerical Analysis of Laminated, Orthrotropic Composite Structures," BRL Contractor Report No. 272, November 1975.* (AD #A018875)

V. CONCLUSIONS AND RECOMMENDATIONS

The SAGA family of codes is operational at BRL and confidence in the programs has been established by test problems. For treating filament wound composite structures, the codes have demonstrated the unique capability of predicting in-laminae shear stresses. The relatively large values of these stresses suggest that they may play a major role in the failure of filament wound composites at wrap angles different from hoop windings. This effect is totally ignored in the SAAS II or similar codes.

The SAGA codes may also handle torsion loading of axisymmetric bodies, another capability not present in SAAS II. The ability to handle torsion loading at the same time as other loadings makes the special purpose torsion code, TORT II[8] developed by the University of Swansea obsolete at BRL.

The factor of 2.5 increase in computer run time of SAGA over SAAS II does not seem too severe a penalty for the additional capabilities gained. The SAAS II code will continue to be used for problems within the scope of that program.

---

[8] *Carson, John and Drysdale, W. H., "An Analysis of Finite Element Code TORT II," BRL Memorandum Report 2463, March 1975.* (AD #A008319)

REFERENCES

1. Sawyer, Stephen Gerard, "BRLESC Finite Element Program for Axisymmetric, Plane Strain, and Plane Stress Orthotropic Solids with Temperature-Dependent Material Properties," BRL Report No. 1539, March 1971. (AD #727702)

2. Zak, Adam R., Second Quarterly Report, Contract No. DAAD05-73-C-0197, Ballistic Research Laboratories, Aberdeen Proving Ground, MD.

3. Zak, Adam R., "Finite Element Computer Program for the Analysis of Layered, Orthotropic Structures," BRL Contract Report No. 158, June 1974. (AD #783412)

4. Zienkiewicz, O. C., Finite Element Method in Engineering Science, McGraw-Hill, New York, 1971.

5. Futterer, Arnold, "Finite Element Analysis of Acceleration Effect on an Internal Ferrule Pressure Gage," forthcoming BRL Memorandum Report.

6. Ashton, J. E., Halpin, J. C., and Petit, P. H., Primer on Composite Materials: Analysis, Technomic Publ, Stamford, Connecticut, 1969.

7. Zak, Adam R., "Numerical Analysis of Laminated, Orthotropic Composite Structures," BRL Contractor Report No. 272, November 1975. (AD #A018875)

8. Carson, John and Drysdale, W. H., "An Analysis of Finite Element Code TORT II," BRL Memorandum Report 2463, March 1975. (AD #A008319)

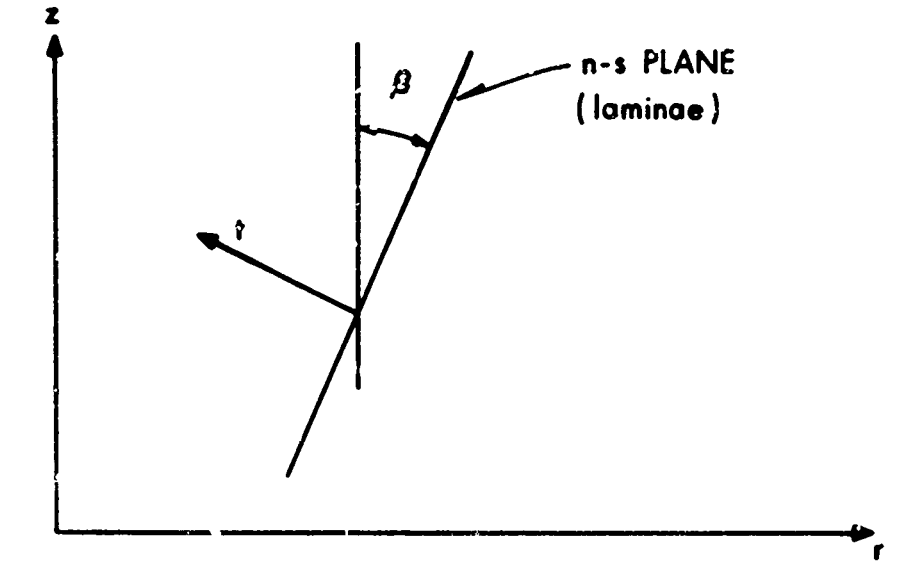

ANGLE β

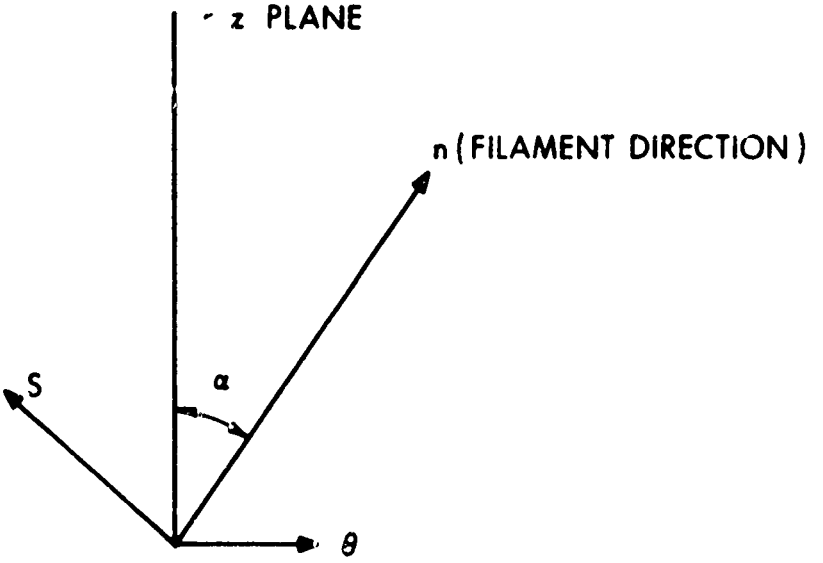

ANGLE α

Figure 1. Orientation of Principal Material Directions to Cylindrical Axes.

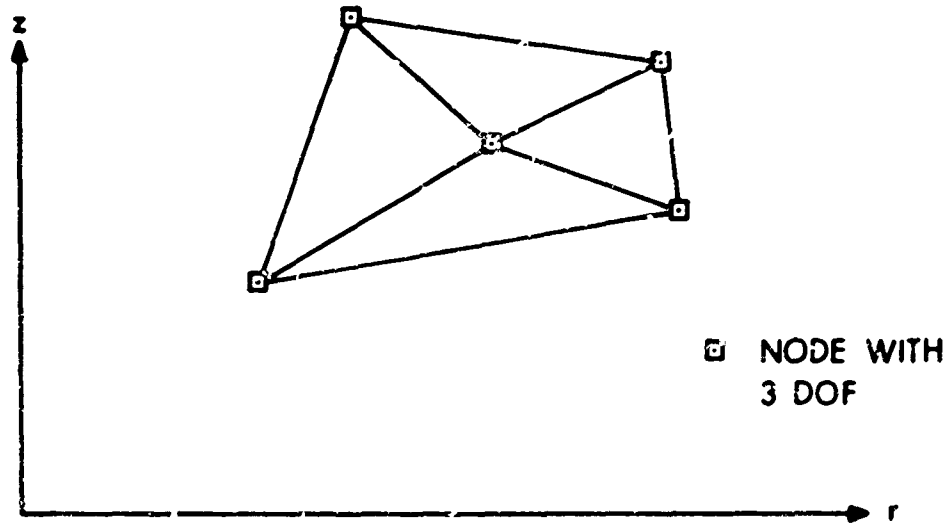

a. SAGA I - linear version

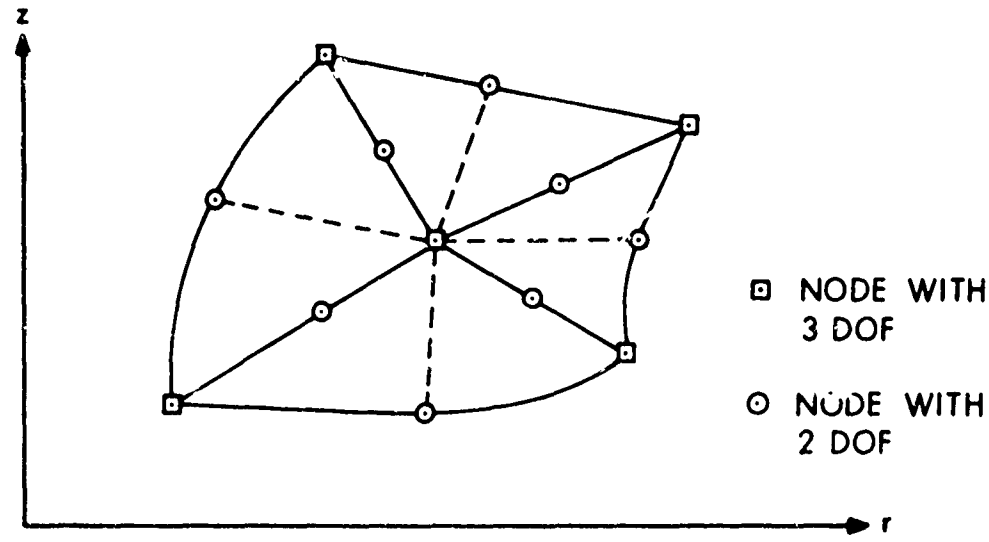

b. SAGA II - quadratic version

Figure 2. Construction of Quadrilateral Finite Element from Triangular Basic Elements.

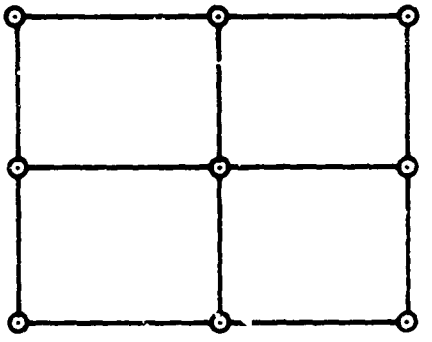

⊙ 3 DOF

a. SAGA I, 27 DOF

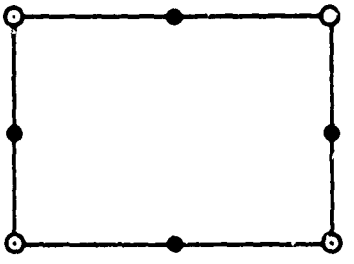

⊙ 3 DOF

● 2 DOF

b. SAGA II, 20 DOF

Figure 3. Nodes and Degrees of Freedom Associated with Final Assembled Elements for SAGA Codes.

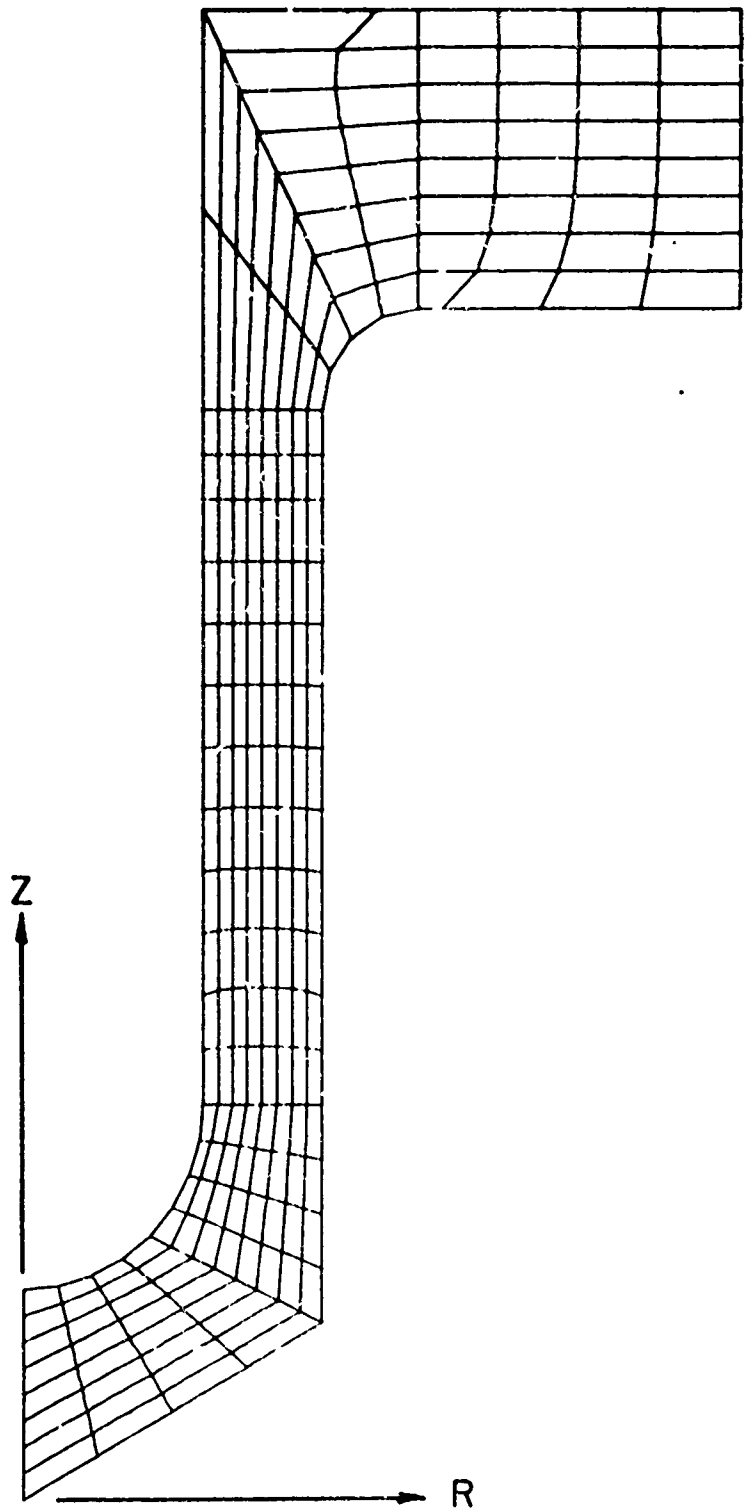

Figure 4. Finite Element Grid for Pressure Gage (from Reference 5).